
# Autonomous Inland Water Monitoring

## *Design and Application of a Surface Vessel*

By Gregory Hitz, François Pomerleau, Marie-Ève Garneau, Cédric Pradalier, Thomas Posch, Jakob Pernthaler, and Roland Y. Siegwart

*Digital Object Identifier 10.1109/MRA.2011.2181771*
*Date of publication: 17 February 2012*

This article presents a novel autonomous surface vessel (ASV) that was designed and manufactured specifically for the monitoring of water resources, resources that are not only constantly drained but also face the growing threat of mass proliferation (bloom) of noxious cyanobacteria. On one hand, the distribution of these blooms in a given water body requires a surveillance of biological data at high spatial resolution on both vertical and horizontal axes, whereas on the other hand, the understanding of the temporal evolution of the cyanobacteria necessitates repeated sampling at the same location. Therefore, our ASV was designed to combine the ability to take measurements within a range of depths, with its custom-made winch, and accurate localization provided by the global positioning system (GPS), without the need for static installations. This article first describes the ASV conception, and then the results of extended field tests on the waypoint navigation mode are discussed. Finally,


1070-9932/12/$31.00©2012 IEEE

the first results of a sampling campaign for monitoring algal blooms in Lake Zurich are presented. This work constitutes advances in the deployment of mobile measurement platforms for environmental monitoring in lacustrine environments. Furthermore, it investigates the application of a single ASV to capture both spatial and temporal dynamics of harmful cyanobacterial blooms in lakes. Combining surface mobility with depth measurements within a single robot allows fast deployments in remote location, which is cost efficient for lake sampling. This reduces the need for fixed installations, which can be impossible in recreational areas. The high-resolution sampling of lakes will contribute to understand and predict the occurrence of harmful cyanobacterial blooms for a better management of water resources.

## Motivation

The monitoring of water resources is of increasing importance as Earth's reservoirs of clean, potable water are drained by an expanding human population, rapid economic growth, and environmental degradation [1]. One emerging threat to freshwater ecosystems is the increasing occurrence of massive development (bloom) of noxious cyanobacteria (blue–green algae) caused by the rising rates of anthropogenic nutrient inputs [2]. These blooms cause a variety of harmful impacts on aquatic ecosystems, either through the depletion of dissolved oxygen in water resulting from the decomposition of the extensive amounts of organic material produced during such blooms or directly due to the production of acutely toxic substances. These cyanotoxins are known to bioaccumulate in aquatic organisms, including fish and mussels [3]. Consequently, cyanobacteria outbreaks result in severe degradation in the water quality, first because large quantities of phytoplankton and/or dead fish give rise to nauseating odors and second because it can even cause cattle and human illness and death [4]. The escalating occurrence of harmful cyanobacterial blooms in fresh waters is likely to intensify due to the global increase of air temperatures [5].

For many lakes, however, the basin-wide variability of these noxious algae at a given season and/or throughout the year is still poorly documented. Current sampling methodologies, e.g., manual water collection by lowering a self-closing 5-L bottle at one specific depth from a small craft, are too time consuming and expensive in terms of manpower to be applied to regular monitoring on a large spatial or fine temporal scale, both for scientific and water management projects.

While extended oceanic observation networks deploy more and more autonomous mobile robots [6], [7], few are used for lake monitoring [8], [9]. None of these deployments has aimed for long-term missions on the order of months or years. Therefore, limnologists are actively looking for solutions to increase the spatial and temporal data acquisitions to improve the monitoring of harmful cyanobacteria and to expand their understanding of lake ecosystems in general.

The newly designed ASV presented here (see Figure 1) allows environmental sampling at temporal and spatial resolutions that are relevant to the variability in lake hydrology as well as in microorganism processes. The vessel, called *Lizhbeth*, is a catamaran (2.5 m long and 1.8 m wide) that has been optimized with respect to efficiency in the forward direction as well as for pitch and roll stability in the presence of waves. Lizhbeth has a differential drive configuration to allow for rotations on the spot that help maneuvers in narrow passages mainly close to the shore. In between the two hulls, we installed a custom-designed winch, which permits to lower an YSI-6600 probe equipped with limnological sensors for adequate lacustrine (related to or associated with lakes) measurements.

## Limnological Aspects

The principal experimental field is Lake Zurich, a very popular recreational area and the major source of drinking water for the city of Zurich. It has an elongated shape of approximately 36 km long and a maximal width of 4 km. This large (66.8 $km^2$) and deep lake (136 m, mean depth of 49.9 m) is subject to the typical seasonal dynamics seen in prealpine lakes, i.e., a summer thermal stratification followed by an winter mixis (physical mixing of the surface and the deep water layers induced by winter winds, which break the vertical stability of the water column as the density gradient between the two layers is gradually reduced because of the cooling of the surface waters). Surface water temperature varies from more than 20 °C in summer to around 5 °C in winter. Lake Zurich as well as other numerous lakes of the Northern Hemisphere that display seasonal stratification are sites of recurrent blooms of the cyanobacteria *Planktothrix rubescens* [3] (see Figure 2). Species within the genus *Planktothrix* are among the most important producers of hepatotoxic microcystins in fresh waters [10], a toxin that strongly inhibits protein phosphatases that may cause serious damage to the liver. Microcystin poisoning of livestock and humans can occur directly through the ingestion of toxic cyanobacterial cells or indirectly through the consumption of contaminated aquatic organisms [3]. Since this toxic cyanobacteria is light sensitive, massive accumulation do not form on the

**Figure 1.** Lizhbeth, the new limnological ASV, during a sampling mission on Lake Zurich. The probe is dragged in the water while moving vertically from the surface to 20 m depth.

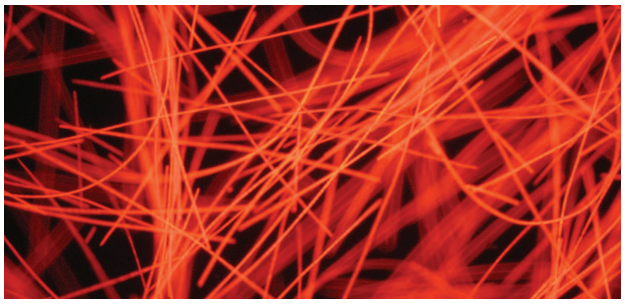

**Figure 2.** *Planktothrix rubescens* (epifluorescence micrograph).

surface but between 5 and 20 m depth in summer and fall periods [11].

The seasonal dynamics of *Planktothrix rubescens* in Lake Zurich have been widely documented over the last few decades (e.g., [11], [12] and other works by Walsby et al.), but measurements have only been taken once a week from vertical profiles made at a single point in this large lake. Even though this provides a fair amount of information to describe dynamics with respect to depth and season, periods of rapid biological changes, such as seen in the springtime, need to be repeatedly sampled at least once a week over a time span in the order of several weeks. Furthermore, the use of such single-point sampling strategy assumes that the population of cyanobacteria is evenly distributed over the entire lake. As documented in previous studies using autonomous sampling robots [8], [9], our preliminary observations of the physicochemical and biological parameters of Lake Zurich suggest that this homogeneity assumption might not hold.

The goal of this work is to collect physicochemical data every two weeks from the surface to 20 m depth, while the ASV is sailing over a transect of 1.5 km that crosses the lake in front of the Limnological Station (University of Zurich, Switzerland). The ASV will allow for high sampling frequency, which is required to study, for instance, the spring period. Moreover, because of its rapid deployment potential, the ASV can also be used to sample punctual meteorological events, such as storms, and thus can be helpful to study the impact of strong winds on *Planktothrix rubescens* abundance and distribution. The winch installed on the ASV is used to make vertical profiling by lowering, while the boat is sailing, a commercial probe equipped with various sensors. The following limnological parameters are measured: temperature, conductivity, dissolved oxygen, photosynthetic available radiation, as well as the fluorescence of two algal pigments, i.e., chlorophyll fluorescence (a proxy for phytoplankton abundance) and phycoerythrin fluorescence (a proxy for *Planktothrix rubescens* abundance). The correct estimation of temporal changes at a given location requires that observations are measured repeatedly along the same fixed transect. This creates another challenge to the ASV navigation, since the platform must sail safely in this busy recreational lake that is also used for public transportation via ferries.

## Related Work

During recent years, the field of autonomous mobile robotics has gained more interest in ASV and autonomous underwater vehicles (AUVs). These systems have a large range of applications as they can access areas that are potentially dangerous for humans. The four most important uses of these platforms are military application [13], structure inspection (particularly in the oil industry), shipwrecks surveys [14], and ecological studies [7], [15]. Most of these projects use AUVs, which always goes along with limited localization methods. Some projects overcome this limitation by combining mobile robots for spatial resolution and static nodes for temporal coverage [7], [9], [16].

Dunbabin et al. [15] have investigated a low-cost, vision-based navigation system for an AUV operating in shallow waters. Even though this system avoids expensive sensors for acoustic localization methods, it cannot be applied in open and deep waters where no visual features are available. Moreover, underwater communication is difficult and allows only for limited transmission rates. Both localization and communication can be achieved easily on surface waters, and therefore more sophisticated applications have been developed. Military and defense applications deploy ASVs to patrol shorelines or harbors. Elkins et al. [13] have assembled an ASV system that operates on relatively large motor boats and possesses a sophisticated set of sensors to detect obstacles or target boats, which can then be followed.

Environmental monitoring projects usually deploy electrically driven ASVs and aim for long-term autonomy because most natural ecosystems change very gradually. Some systems [17] also employ solar panels to extend their maximal autonomy range. In such applications, ASVs are often operated in a waypoint navigation mode, which allows them to travel along predefined paths. Results of such waypoint navigation tasks are presented in several publications [9]. Dhariwal and Sukhatme [18] discuss a dynamic model for the localization of an ASV by fusing sensor inputs and a controller for waypoint navigation that was tested on a small lake. Zhang and Sukhatme [16] proposed an adaptive sampling algorithm that takes into account the energy consumption of the mobile surface robot. The mobile robot communicates with static nodes, acquires sensor readings from them, and then tries to optimize its path to minimize interpolation errors. This type of sampling is very energy efficient, but fixed buoys are needed to properly plan a path, which requires installation time and may raise legal issues with the local authorities.

Measurements taken using floating vessels are usually restricted to the surface, which is suitable to study the ocean–atmosphere interactions [19]. However, this layer represents only a minor portion of the global ocean and thus, phenomena occurring underwater are overlooked. To our knowledge, only the ASV constructed by Dunbabin

et al. [20] is able to take measurements at depths down to 5 m while moving. The Aquatic Networked InfoMechanical System (NIMS-AQ), developed by Stealey et al. [21], is capable to measure at deeper positions; however, its motion is restricted to straight lines. Given that toxic cyanobacteria can be found as deep as 20 m [11], a much larger depth range is required. The ASV developed by Smith et al. [7] has the capability to perform vertical profiling at a fixed location using a sensor attached to a winch system. They developed and tested on the field a station-keeping algorithm that can maintain the ASV on station within 2 m of the desired location under moderate wind conditions (2.5 m/s). This gives a great spatial coverage on the vertical axis, but horizontal variations are not readily evaluated. To assess the variations on both vertical and horizontal axes in a relatively short time span, we designed an ASV to carry a custom-made winch so that it can take measurements as deep as 130 m while sailing to realize a cross-sectional measurements in the lake.

## Designing and Manufacturing the ASV

Our custom-made ASV has been designed and tailored for its application in lakes. Figure 3 shows a computer-aided design (CAD) rendering of the entire system. Its catamaran configuration allows for the winch to be placed centric between the two hulls. The two motors are protected by aluminum sheets, which is important as the cable connecting the probe to the winch passes in between the hulls. The vessel was conceptualized following a bottom–up logic. First, the probe holder was designed; then, knowing the necessary parameters, the winch was constructed. The catamaran was engineered in the last step, i.e., when all variables were known (e.g., dimensions and weights of winch, probe, and electronic parts). The following sections give insights into both the mechanical design and the commercial components of the boat and explain the software design and the modes of operation of the boat.

### *Probe*

In this work, an YSI 6600 probe is used to measure limnological parameters. This probe has a cylindrical shape and an attachment point on one end. Therefore, its axis is aligned vertically in steady state. However, if it is moved horizontally, large drag forces will let it diverge from the vertical. In this work, we refer to the angle of the cable at the water surface with respect to the vertical as drag angle. For the application in the scope of this project, two criteria are important. First, the probe should create minimal drag while it is pulled through water and second, it is desirable that the horizontal displacement of the probe with respect to the boat is minimal. This eases the estimation of the position of the probe, which is crucial to prevent it from hitting the floor. To fulfill these two requirements, we have considered the following design concepts. The drag force that is created by the probe can be minimized by placing the probe horizontally. This was achieved by shifting the attachment point of the cable to the center of gravity of the probe. Furthermore, a projectile-like tip of the support structure [see Figure 4(a)] ensures an optimal flow field at the tip of the probe. The horizontal displacement of the probe is a result of the ratio of downward forces (mainly, gravitational forces) and horizontal forces (hydrodynamic forces). The only way to alter this ratio is to increase downward forces on the probe, as the drag force has been minimized already and the forces along the cable cannot be influenced. Our solution to this is twofold. On one hand, we added weight to the probe in the form of a 4.2 kg steel tip. Furthermore, wings were mounted onto the support structure to create a lift force in downward direction and thus decrease the horizontal displacement further. Following these optimizations, the hydrodynamical design of the probe casing is a fiberglass tube with flat fiberglass wings and a 4.2 kg steel tip in front [see Figure 4(a)]. The probe can be inserted into the tube from the rear end. Fiberglass was chosen because a thin and rigid material was needed to preclude any influence on the water circulation to the sensor at the probe front.

**Figure 3.** CAD rendering of the final design of the ASV.

Several test iterations were made in a water channel during which the probe was pulled at 1 m/s in the horizontal direction. The cable length was fixed to 1 m. When only the probe without the support structure was dragged, a drag angle of 71° was measured. The tests with the support structure showed that the drag angle could be reduced to 6.8°.

### *Winch*

A winch was required to lower the probe to different depths. A cable of up to 130 m in length is needed to cover the maximal depth of Lake Zurich and therefore requires the winch to support its weight. The winch system should also provide a mechanism to lift the probe out of the water to operate safely in shallow regions and to allow users to remove or attach the probe easily. Another requirement is the ability to transfer the measured data directly to the onboard computer of the boat by the use of a slip ring. As such a specialized winch system was not available commercially, it required a custom design. Figure 4(b) shows a rendering of the final design of the winch. It consists of the cable's drum, where the cable is wound up, the lifting arm

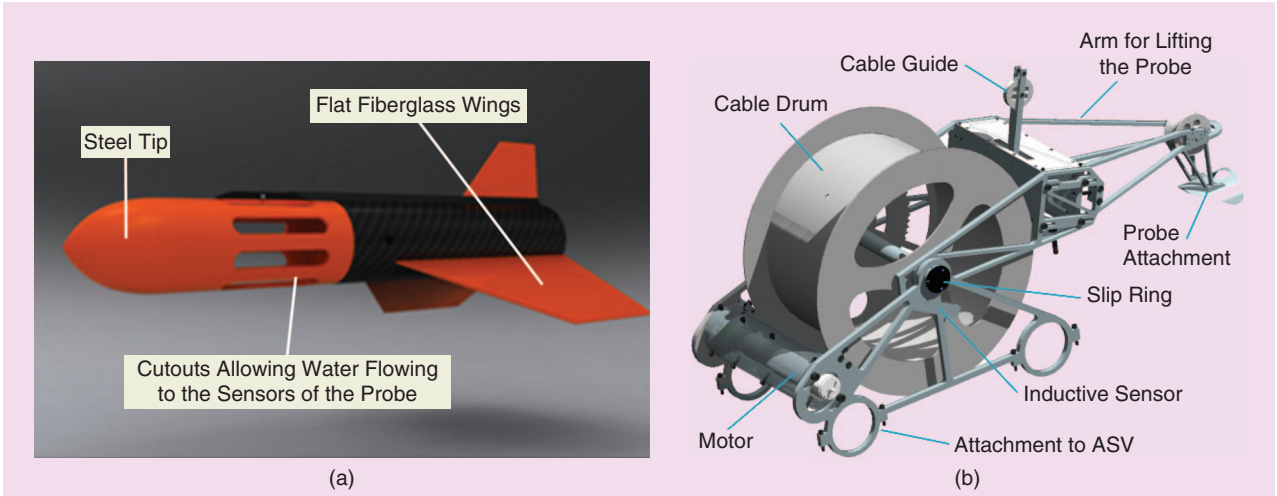


**Figure 4.** CAD rendering of the (a) probe support structure and (b) winch system, respectively.

that lifts the probe out of the water for ease of access, a cable guide to avoid knots when winding the cable up, a slip ring for communication purposes, and the motor and motor controller for actuation.

The whole winch is made of stainless steel, rust proof bearings, and aluminum to enable outdoor operation without cover. To lift the arm with the probe out of the water into the parking position, the motor uses a maximum force of 15 N·m. For this purpose, a Maxon RE40 motor was chosen with a planetary gear head providing a gear transmission ratio of 1:156. To detect the arrival of the probe at the parking position, an inductive sensor indicates when the arm is raised to an angle of 60° to the horizontal. At this angle, the probe is comfortably removable.

### The Hulls

A standard catamaran has a smaller bow and a wider stern. The wider stern counteracts the dynamic buoyancy effects that occur at higher speeds. However, at lowers speeds, the wide stern causes more turbulence and thus more drag. We have chosen a symmetrical bow and stern configuration since the ASV is not targeted to go faster than 1.5 m/s. At this speed, dynamic buoyancy is negligible. Furthermore, the symmetrical configuration has another advantage: only one positive and one negative mold are required to laminate the two halves of one hull.

To design the shape of the hulls, three concepts were used that are common in ship hull design: 1) Bezier curves, 2) the prismatic coefficient, and 3) the desired buoyancy. Whereas Bezier curves produce smooth surfaces that only create little turbulence [22], the prismatic coefficient characterizes the pitch behavior and therefore the steadiness of the boat in the presence of waves. For the calculation of the desired buoyancy, the minimum and maximum expected weights were set to a minimum and maximum water level. At a minimum weight of 120 kg, the ship propellers still have to be underwater. The maximum weight was set to 340 kg, which is what can be expected with additional components and a person standing on the ASV. The hulls consist of four identical hull halves laminated inside a fiberglass negative mold. Lightweight construction was achieved with a foam core layer strategy. The flotage includes a gel coat for UV protection. The underwater part is painted with an antifouling finish.

The motors are integrated in the center of the hulls. No rudders are needed since steering is done by different motor rotating speeds. In the middle of the hull, the motor propellers are protected with an aluminum sheet against collision. The risk of human injury is thereby reduced and contact with the cable to the probe is prevented.

### Components

This section gives a brief overview of the electrical components, sensors, and actuators. The boat is propelled by two standard electrical boat motors (Yamaha M12) and two lead acid batteries (12V, 70 Ah), which are situated in one of the hulls each. The Helios development kit (by Diamond Systems) was chosen for computing purposes. Additionally, a second board (pITX-SP 2.5 in single-board computer), which features an Atom Z510 processor, is installed for higher-level computations. Localization is achieved via a GPS module and a magnetic compass. The GPS coordinates are accurate enough for limnological purposes ($\pm 5$ m); therefore, differential GPS is not considered. An active single beam depth sonar from CruzPro is used to measure the water depth and prevent the probe from hitting the ground. The boat features a wireless network that allows for system monitoring from a laptop and for remote control via a joystick.

### Software Design

The software that has been developed to operate the ASV is based on the robotic operating system (ROS)

(http://www.ros.org). It gives advantages of the many features and useful tools that are available along with this versatile middleware. The low-level components of the system, such as hardware driver nodes, are not detailed in this article.

The system can be operated in either remote-controlled (RC) mode or in autonomous mode. In the RC mode, signals from a joystick are generating the commands to the propulsion and winch motors. In the autonomous mode, a hierarchical control structure with three main levels is implemented: 1) low level controllers, 2) actuator synchronization, and 3) mission management. On the low level 1), the two main actuators of the boat, namely the propulsion system and the winch, are designed as action servers in the ROS framework. Whereas the winch controller supports simple control for positioning the probe at arbitrary depth levels and controls the vertical speed of the probe, the propulsion system provides a waypoint navigation system, which allows the boat to travel along predefined paths at constant speed. A path is composed of line segments, which serve as input to the line-following controller. It is based on a two level-controller that uses a PID-controller to keep the boat speed constant on a first level. On top of that, a line-following controller is used to control the boat position with respect to the predefined target line. It bases on the control scheme presented by Samson and Ait-Abderrahim [23] and has been extended with an integral term to account for external perturbations. In the following equations, $\varphi$ denotes the error in heading with respect to the target heading of the line segment, $d$ is the distance between the boats current position and the closest point on the target line, $v$ is the current speed of the boat, and $v_r$ is the desired speed. $p_{th}$ denotes the thrust level (in percentage of motor power), whereas $p_{tu}$ is the turn level.

$$p_{th}(t) = \mathrm{PID}(v(t) - v_r, t),$$

$$p_{tu}(t) = k_{p\varphi}\varphi(t) + \frac{\sin\ \varphi(t)}{\varphi(t)}\left[-k_{pd}d(t) + k_{Id}I_d(t)\right]p_{th}(t),$$

$$I_d(t) = \int_0^t d(\tau)d\tau.$$

The additional integrated term $I_d$ enables the controller to handle constant external perturbation forces generated by wind or water currents. The parameters of the controller have been fine tuned and validated on water. A validation of the proposed control strategy is provided in the "Controller Dynamics" section. On the intermediate level 2), another action server is used to enable the winch and the propulsion system to execute synchronized actions, which is necessary to use the probe at changing depth levels in between two consecutive waypoints. The services provided by these three action servers can then be called by a mission script, which runs on the high level 3). Mission scripts can be uploaded in a convenient manner via a Web server that runs on the boat. Mission scripts are written in Python, which allows decision making (if structures) and repetitions (while and for loops). Google Earth can be used to generate waypoint-based paths.

### Sampling Strategy

As mentioned previously, the series of measurements taken over several decades in Lake Zurich ([12] and other work by Walsby et al.) do not inform on the horizontal distribution and the fine temporal dynamics of *Planktothrix* blooms. Therefore, the deployment of the ASV is configured to increase the resolution of the field samplings.

During the first sampling campaign, starting from October 2010 to September 2011, the ASV collected data along a straight line (1.5 km) across the lake. While the boat travels from one side of the lake to the other, the probe is being lowered and pulled up between two predefined depth levels (usually 3–20 m). The vertical and horizontal motions of the probe result in a zigzag-shaped trajectory that provides a series of data points within a vertical plane across the lake (see Figure 5). The probe provides measurements at 0.5 Hz only; thus; it must travel at slow speed to get as many measurements as possible. Consequently, the boat speed was set to 0.7 m/s, whereas the vertical speed of the probe was set to 0.1 m/s. The choice of these parameters is based on the stratification of the water body and hardware-related constraints: The vertical speed is at its maximal level to maximize the number of zigzags along the line. The horizontal speed is chosen as slow as possible to ensure the capacity of the batteries to last for the entire mission. In a postprocessing step, two-dimensional (2-D) interpolation methods can be applied to the data to generate a cross-sectional representation of the measured data. Given the large difference in the scale of the horizontal (1.5 km) and the vertical axes (~20 m), the 2-D interpolation is computed using an anisotropic distance kernel. This kernel weights data points inversely proportional to their Euclidean distance and applies a weighted average to 5% of the data points with the highest weights. Prior to that, the field is scaled by a factor of 200 m in horizontal distance to account for the difference in scale. The accurate GPS-based waypoint navigation system of the ASV guarantees the repeatability of the

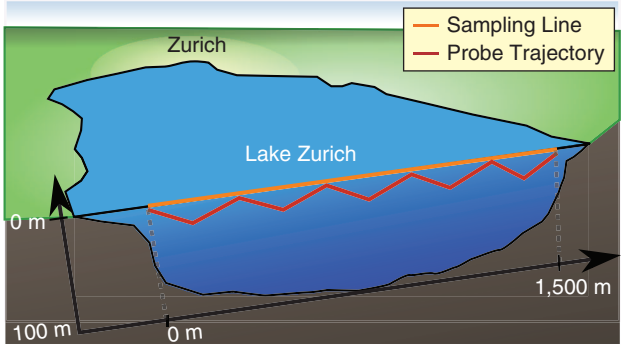


**Figure 5.** A schematic illustration of transect sampling strategy. The probe is lowered and pulled up between two predefined depth levels along a path across the lake.

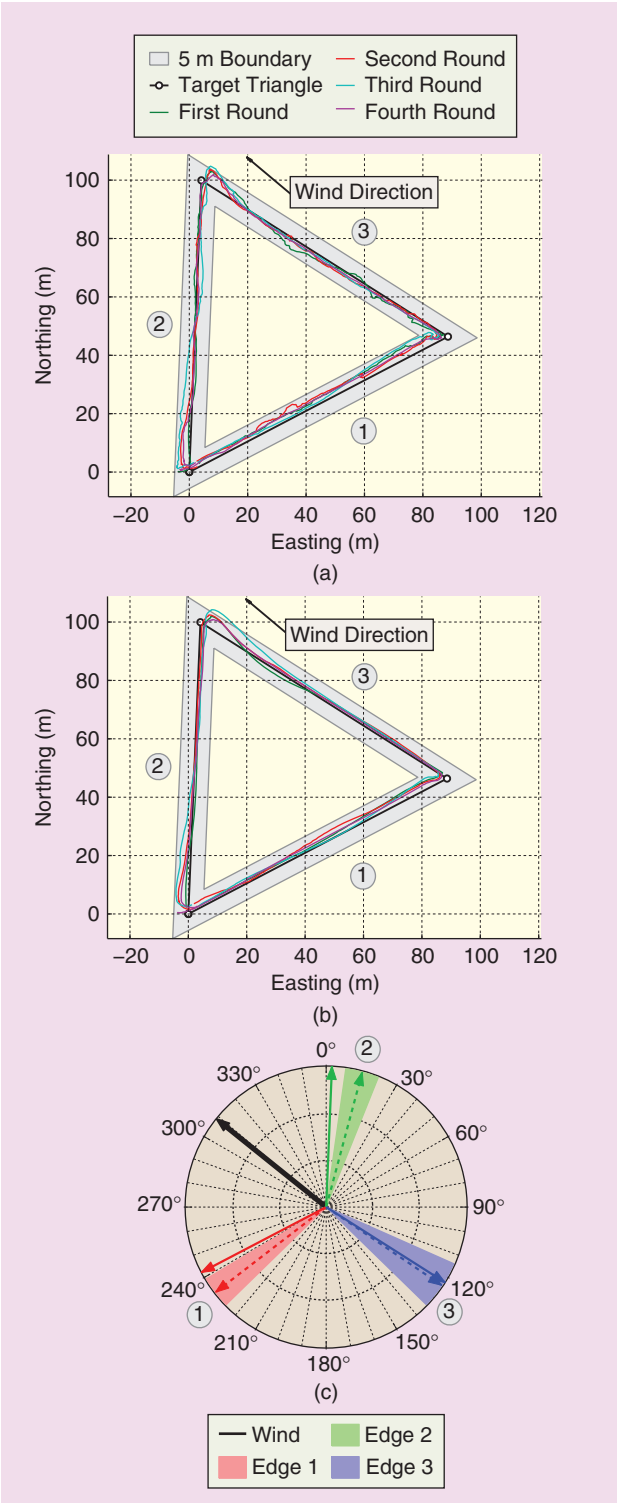


**Figure 6.** A comparison of the traveled path tracked by (a) GPS and (b) theodolite measurements. In the third plot (c) compass data are depicted in comparison to the target headings of the triangle edges. The boat traveled in clockwise direction.

measurements with respect to position and allows the comparison of transect data sets over time. Examples of the data collected during the transect missions are presented in the "Analysis of Sampled Data Sets" section.

## Results

### *Controller Dynamics*

The performance of the line-following controller was evaluated experimentally. The data set was recorded while the ASV traveled along a predefined equilateral triangle of 100-m side length for a total of four rounds. During this test, the line-following controller was utilized as presented in the "Software Design" section. The target velocity was set to 0.7 m/s for all rounds, i.e., the speed used during the transect sampling missions. The three corner points of the triangle shown in Figure 6 define lines that were sent to the line-following controller. The target triangle and the traveled path of the boat can be seen in Figure 6(a).

From the plotted data, it is evident that the controller converges to the desired line. The stability of the controller was proved by Samson and Ait-Abderrahim [23]. The plotted data shows smooth and quick transitions between different segments of the path. While the boat is rotating on the spot (i.e., on all three corners of the triangle) to point toward the new target point, the position is not actively controlled and thus the boat drifts due to wind. Table 1 shows the average distance and the standard deviation from the target lines of the triangle accumulated over the four rounds.

In addition to the internal GPS measurements, an external system has been used to track the boat position. A laser-based theodolite by Leica (TS15) capable of tracking a prism to a distance of up to 2 km with an accuracy of 4.5 mm has been set up at the shore as an external positioning system. A calibration procedure has been applied to estimate the transformation from the local frame of the theodolite to the global reference frame. It is based on the *libpointmatch* library [24] that implements an iterative closest point (ICP) algorithm.

Figure 6(a) and (b) show the recordings of the GPS locations and the theodolite measurements, respectively. From the theodolite measurements, it can be seen that the desired path is achieved, despite the noise on the GPS signals. Furthermore, the plots show a 5-m boundary area that the boat should not leave to achieve the desired precision for the biological sampling missions. The GPS measurements show an RMS error of 1.29 m with respect to the theodolite measurements. It is important to note

**Table 1. Average lateral error from target lines and the corresponding standard deviation.**

| Triangle Side | Average Error (m) | Standard Deviation (m) |
|---|---|---|
| First triangle edge | 0.62 | 1.49 |
| Second triangle edge | 0.04 | 1.98 |
| Third triangle edge | −1.63 | 2.69 |

that this value depends on the ICP procedure that is used to estimate the transformation between the theodolite and GPS measurements.

During the test, strong winds blew (average speed: 5 m/s with gusts of up to 15 m/s). The wind measurements were not acquired online on the boat, but were available from a meteorological station close by. The plot in Figure 6(c) shows the target heading along each of the three edges (solid arrows) and the mean of the compass measurements (dashed arrows). The shaded areas depict a band ±3 times the standard deviation. The black arrow shows the direction of the wind. Especially on the edges 1 and 2, it can be seen that the boat was compensating for the perturbation caused by wind. The mean heading of the boat is approximately 10° off from the target heading.

Along with the accuracy of the line-following controller, the speed controller has also been evaluated. Figure 7 indicates the deviation of the actual speed from the target speed during the triangle test. The numbering of the line segments corresponds to the chronology of the three edges of the triangle during the four rounds. The box plot shows that the median of the speed values is very close to the desired target value. The large amount of outliers is due to the noise level of the speed readings that are provided by the GPS device.

This evaluation shows that our ASV is capable of very accurate GPS waypoint navigation in the presence of high external perturbations. On the spot, rotations enable smooth transitions between consecutive segments of the path, even if they differ largely in direction.

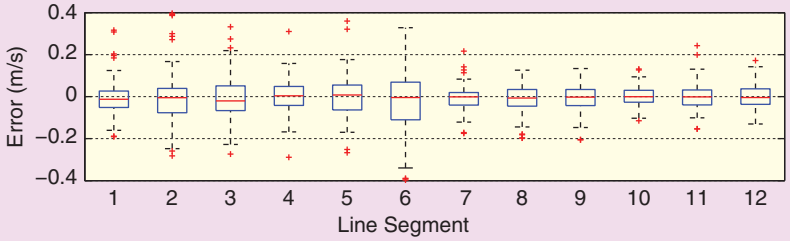


**Figure 7.** Errors of the measured speed of the boat with respect to the desired target speed (0.7 m/s). The speed measurements are provided by the GPS device.

## *Probe Localization*

The laboratory experiment described in the "Probe" section has shown that the wing configuration of the probe support structure significantly decreases the drag angle. However, these tests were restricted to a cable length of 1 m due to the depth of the water channel. To evaluate the drag behavior when using longer cable lengths, we have done a series of tests in the lake. Figure 8 shows an example of the recorded data. The upper part of the plot compares the measured depth of the probe and the corresponding length of the cable. The lower plot indicates the speed of the boat when sailing along a straight line. The target speed for the controller has been set to 0.6 m/s. During transition between different depth levels, the boat stopped, causing a transient phase until the desired speed level has been reached for the next section of the test. The gray areas indicate the steady-state phases from which the data have been extracted for further analysis. To estimate the drag in the horizontal direction and the drag angle from these measurements, the following equations provide the worst-case estimate in which the cable is assumed to be a straight line:

$$dx = \sqrt{l^2 - d^2}, \qquad \alpha = \arccos\left(\frac{d}{l}\right).$$

The displacement of the probe in the horizontal direction with respect to the boat is denoted by $dx$, $l$ corresponds to the cable length, $d$ is the depth measured by the probe, and $\alpha$ denotes the estimated drag angle.

Table 2 shows the resulting mean values for the four steady-state phases that are indicated in Figure 8. From these results, several conclusions can be drawn. First, the expected dependency of the drag behavior on the cable length evidently occurs. Second, the results showed provide a simple model to estimate a worst-case estimate of the drag in the horizontal direction, which enables the

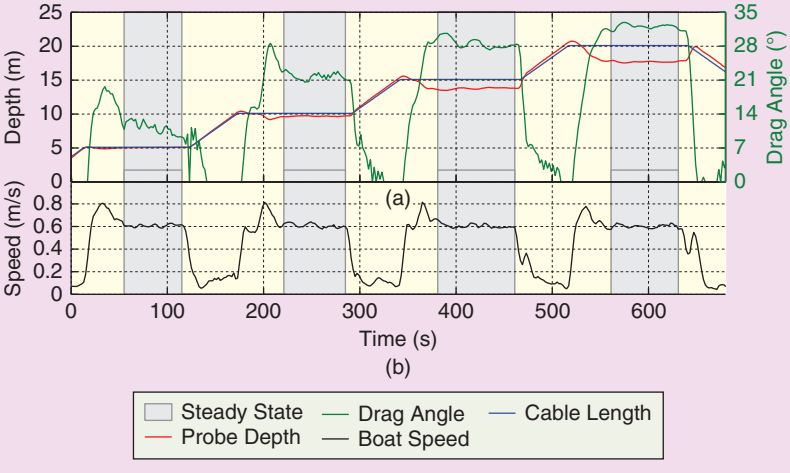


**Figure 8.** (a) shows a comparison of cable length and the depth measured by the probe. (b) shows the travel speed of the boat (GPS measurements). The gray areas indicate the steady-state phases.

**Table 2. Average values for the steady-state phases of the drag estimation data set (compare Figure 8).**

| *l* (m) | *dz* (m) | *dx* (m) | α (°) |
|---|---|---|---|
| 5.00 | 0.10 | 0.96 | 11.13 |
| 10.00 | 0.72 | 3.72 | 21.82 |
| 15.00 | 1.84 | 7.19 | 28.63 |
| 20.00 | 3.06 | 10.63 | 32.09 |

localization of the probe within the given noise level of the GPS readings. In the current sampling campaign, the boat is asked to sample up to 20 m along a 1.5-km line. For this application, the maximal localization error of the probe is 0.6% in the forward direction.

### Analysis of Sampled Data Sets

Since September 2011, 15 sampling missions have been carried out on Lake Zurich according to the sampling strategy described in the "Sampling Strategy" section. Since the target sampling line is 1.5 km long and is covered twice per mission, a total distance of 45 km has been covered in the autonomous waypoint navigation mode. During each mission, six parameters are measured across the transect plane. This yields 180 interpolated plots, which allows biologists to draw first conclusions and have raised their interest in future applications of the platform. Figure 9 shows four examples of such cross-sectional data profiles. The black lines indicate the trajectory of the probe. The upper two plots show the temperature distribution within the transect plane. Besides the vertical thermal stratification of the water column, which is a common feature of lakes in temperate areas during spring and summer, horizontal gradients in temperature can also be perceived. The temperature fields yielded by the two consecutive passes (i.e., transect 1 versus transect 2) along the exact same sampling line display some differences. These changes have occurred within 1 h and might be related to internal seiche movements (standing waves within the water body). Even though they are well assumed, these physical dynamics have never been documented before in Lake Zurich, despite the fact that they constitute a critical factor explaining the cyanobacteria distribution.

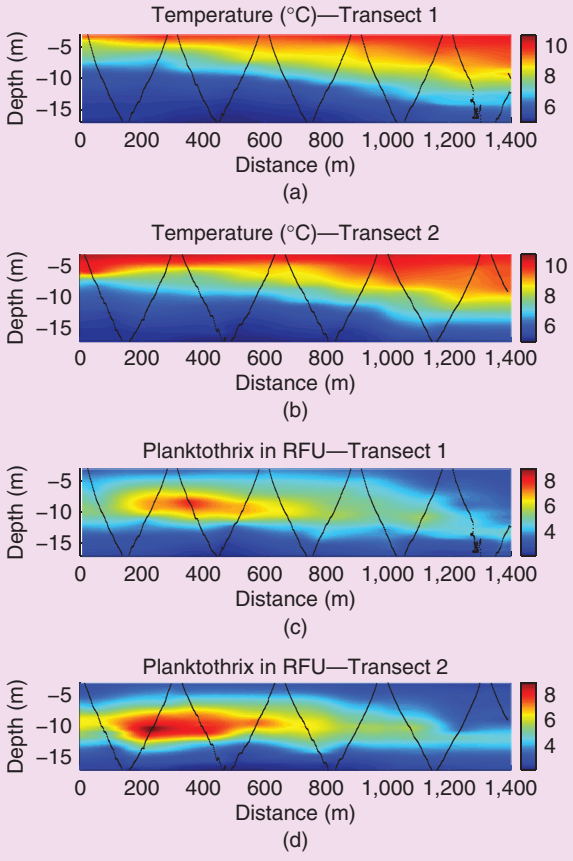


**Figure 9.** (a) and (c) show the resulting temperature field within the transect plane for two consecutive passes (approximately 1 h temporal difference). (b) and (d) show the corresponding abundance of *Planktothrix* cyanobacteria in water.

Figure 9(c)–(d) depicts the distribution of the *Planktothrix* cyanobacteria. Again, the left and right sides of the lakes are different. This substantial spatial heterogeneity indicates that Lake Zurich is not a homogeneous water body, and thus subsequent sampling should account for these local variations. Moreover, the core of the *Planktothrix* patch seemed to have moved 2 m downward between transects 1 and 2, showing once more the rapidity of changes taking place in the lake. This means that our platform should be able to capture physical variations that occur at the scales of hours. To gain further insights into this intriguing spatiotemporal distribution of *Planktothrix* population, a high-frequency field sampling (one week, twice a day) was carried out.

### Evaluation of Interpolation Procedure

The interpolated data representation used in Figure 9 is created from relatively sparse points, and therefore a validation is required to get an estimate of the achieved accuracy. The data set presented in Figure 10 is composed of two phases: a vertical zigzag trajectory (phase 1) and lines at constant depth (phase 2). The data from phase 1 (depicted in black) was used to generate an interpolation over the entire region of the plot. The data from phase 2 (shown in blue) served as a reference to which the interpolated values were compared. Each reference value was compared to the closest interpolated value. The box plot on the right-hand side of Figure 10 shows the errors for each line. For each of the measured channels, the error was computed relative to the range of the channel. In Figure 10, only data from one channel are shown, as the errors of all channels are similar. Even though the results in the upper region of the test show very small errors, the lower section has higher errors. This should be kept in mind when

drawing conclusions from the interpolated plots. However, it has to be noted that the reference lines were recorded in a top to bottom manner, and therefore the time difference between the interpolation data 1) and the reference 2) is highest at the bottom (approximately 1.3 h). To compare the error of the interpolation to the temporal variability of the field, we computed two rms values. The first one reflects the differences of the interpolated values to the reference points (10.23%). The second one compares the raw data points used for interpolation (black) to the closest reference point (13.21%). The comparison of these two values shows that the error of the interpolation lies within the temporal variability of the field.

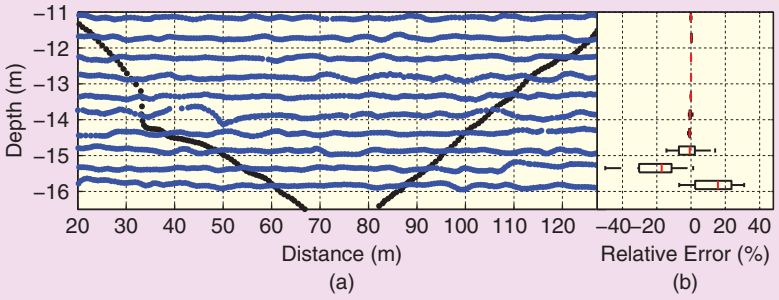


**Figure 10.** (a) shows the data used for interpolation (black) and measurements on horizontal lines for validation (blue). (b) shows the error of the interpolated values with respect to the range of the entire data set.

## Conclusion

This article presents the design of a surface vessel for the autonomous monitoring of water bodies and its validation over a year of field testing. Three main design aspects are presented in detail to show that the platform has been specifically tailored to suit the desired applications. First, the platform has been manufactured with lightweight materials resulting in a total weight of 120 kg, which includes 40 kg of batteries. This allows the platform to be deployed in remote locations without the need for specialized infrastructure.

Second, special attention has been drawn to minimize the probe drag while being pulled below the boat. When using the depth measurement provided by the probe in combination with the known length of the cable, we can assure a reasonable localization of the probe. Even assuming a worst-case scenario, we showed that the error on the estimate of the probe displacement in the horizontal direction is relatively small compared to the total travel distance of the actual sampling missions. We intend to develop in the near future a better model to reduce the resulting error.

Finally, to achieve smooth waypoint navigation, we implemented a simple, still robust control algorithm that ensures an accurate and repeatable line-following motion with lateral errors being smaller than 2 m, cross-validated using a very precise external positioning system. The waypoint navigation is the core of the mission planning system of the platform, which is straightforward enough so that biologists can easily operate it. The mission planning can be adapted to the specific needs of the biologists and was successfully used to conceive efficient sampling campaigns.

All these design considerations gave rise to a system capable of obtaining reliable long-term localization for repeated sampling at the exact same position to observe the temporal evolution of a given aquatic ecosystem as well as increasing the spatial coverage on both vertical and horizontal axes. Our project can be seen as a small-scale sensor network that combines temporal and spatial resolutions, which is often more convenient and cost efficient for lacustrine sampling. Moreover, it is worth mentioning that our system is not restricted to lake sampling because the control functions as long as wind speed is lower than 15 m/s.

Our first measurements in Lake Zurich support the assumptions that this water body displays a strong horizontal heterogeneity in its physicochemical parameters and that these parameters can change relatively fast. These observations raised the need for further investigations on the dynamics of *Planktothrix* populations. For these reasons, we are routinely deploying the ASV to complement the ongoing sampling campaign of Lake Zurich that is performed with traditional limnological techniques. We also plan to develop an adaptive sampling framework in which measurements are analyzed online such that the layers of interest can be sampled at a higher frequency. Furthermore, measurements of prior missions could be used to target specific sampling areas. Another sampling scheme would be to detect patches of *Planktothrix* along a transect across the lake and then to explore their spatial extent in three-dimensional space.

## Acknowledgments

This work is funded by the Swiss National Science Fund (CR22I2-130023). The authors thank Manuel Baumann and Oliver Baur for their construction efforts and Eugen Loher for his constant technical support.

## References

[1] World Water Assessment Programme, "The United Nations world water development report 3: Water in a changing world", UNESCO, Earthscan, Paris, London, Tech. Rep., 2009.

[2] J. Heisler, P. Glibert, D. Burkholder, J. Anderson, W. Cochlan, W. Dennison, Q. Dortch, C. Gobler, C. Heil, E. Humphries, A. Lewitus, R. Magnien, H. Marshall, K. Sellner, D. Stockwell, D. Stoecker, and M. Suddleson, "Eutrophication and harmful algal blooms: A scientific consensus," *Harmful Algae*, vol. 8, no. 1, pp. 3–13, 2008.

[3] K. Sivonen and G. Jones, "Toxic cyanobacteria in water: A guide to public health significance, monitoring and management," in *Cyanobacterial Toxins*, I. Chorus and J. Bertram, Eds. London: E&FN Spon, 1999, pp. 41–111.

[4] G. Codd, J. Lindsay, F. Young, L. F. Morrison, and J. Metcalf, "Harmful cyanobacteria," in *Harmful Cyanobacteria—From Mass Mortality to Management Measures*, J. Huisman, H. C. P. Matthijs, and P. M. Visser, Eds. Dordrecht: Springer-Verlag, 2005, pp. 1–23.

[5] K. Johnk, J. Huisman, J. Sharples, B. Sommeijer, P. Visser, and J. Stroom, "Summer heatwaves promote blooms of harmful cyanobacteria," *Global Change Biol.*, vol. 14, no. 3, pp. 495–512, 2008.

[6] S. Kröger, E. Parker, J. Metcalfe, N. Greenwood, R. Forster, D. Sivyer, and D. Pearce, "Sensors for observing ecosystem status," *Ocean Sci.*, vol. 6, no. 4, pp. 765–798, 2009.

[7] R. Smith, J. Das, H. Heidarsson, A. Pereira, F. Arrichiello, I. Cetinic, L. Darjany, M.-E. Garneau, M. Howard, C. Oberg, M. Ragan, E. Seubert, E. Smith, B. Stauer, A. Schnetzer, G. Toro-Farmer, D. Caron, B. Jones, and G. S. Sukhatme, "The USC Center for Integrated Networked Aquatic PlatformS (CINAPS): Observing and monitoring the Southern California Bight," *IEEE Robot. Automat. Mag. (Special Issue on Marine Robotic Systems)*, vol. 17, pp. 20–30, Mar. 2010.

[8] D. A. Caron, B. Stauffer, S. Moorthi, A. Singh, M. Batalin, E. A. Graham, M. Hansen, W. J. Kaiser, J. Das, A. Pereira, A. Dhariwal, B. Zhang, C. Oberg, and G. S. Sukhatme, "Macro-to fine-scale spatial and temporal distributions and dynamics of phytoplankton and their environmental driving forces in a small montane lake in southern California, USA," *Limnol. Oceanogr.*, vol. 53, no. 5, pt. 2, pp. 2333–2349, 2008.

[9] G. S. Sukhatme, A. Dhariwal, B. Zhang, C. Oberg, B. Stauffer, and D. A. Caron, "Design and development of a wireless robotic networked aquatic microbial observing system," *Environ. Eng. Sci.*, vol. 24, no. 2, pp. 205–215, 2007.

[10] R. Kurmayer and M. Gumpenberger, "Diversity of microcystin genotypes among populations of the filamentous cyanobacteria *Planktothrix rubescens and Planktothrix agardhii*," *Mol. Ecol.*, vol. 15, no. 12, pp. 3849–3861, 2006.

[11] S. V. den Wyngaert, M. M. Salcher, J. Pernthaler, M. Zeder, and T. Posch, "Quantitative dominance of seasonally persistent filamentous cyanobacteria (*Planktothrix rubescens*) in the microbial assemblages of a temperate lake," *Limnol. Oceanogr.*, vol. 56, no. 1, pp. 97–109, 2011.

[12] A. Walsby and F. Schanz, "Light-dependent growth rate determines changes in the population of *Planktothrix rubescens* over the annual cycle in Lake Zürich, Switzerland," *New Phytol.*, vol. 154, no. 3, pp. 671–687, 2002.

[13] L. Elkins, D. Sellers, and W. R. Monach, "The Autonomous Maritime Navigation (AMN) project: Field tests, autonomous and cooperative behaviors, data fusion, sensors, and vehicles," *J. Field Robot.*, vol. 27, no. 6, pp. 790–818, 2010.

[14] B. Bingham, B. Foley, H. Singh, R. Camilli, K. Delaporta, R. Eustice, A. Mallios, D. Mindell, C. Roman, and D. Sakellariou, "Robotic tools for deep water archaeology: Surveying an ancient shipwreck with an autonomous underwater vehicle," *J. Field Robot.*, vol. 27, no. 6, pp. 702–717, 2010.

[15] M. Dunbabin, P. Corke, and G. Buskey, "Low-cost vision-based AUV guidance system for reef navigation," in *Proc. IEEE ICRA*, 2004, vol. 1, pp. 7–12.

[16] B. Zhang and G. Sukhatme, "Adaptive sampling for estimating a scalar field using a robotic boat and a sensor network," in *Proc. IEEE ICRA*, Roma, Italy, 2007, pp. 3673–3680.

[17] J. Higinbotham, J. Moisan, C. Schirtzinger, M. Linkswiler, J. Yungel, and P. Orton, "Update on the development and testing of a new long duration solar powered autonomous surface vehicle," in *Proc. OCEANS 2008*, PQ, Canada, 2008, pp. 1–10.

[18] A. Dhariwal and G. Sukhatme, "Experiments in robotic boat localization," in *Proc. IEEE/RSJ IROS*, San Diego, CA, 2007, pp. 1702–1708.

[19] M. Caccia, R. Bono, G. Bruzzone, E. Spirandelli, G. Veruggio, A. M. Stortini, and G. Capodaglio, "Sampling sea surfaces with SESAMO: An autonomous craft for the study of sea–air interactions," *IEEE Robot. Automat. Mag.*, vol. 12, no. 3, pp. 95–105, 2005.

[20] M. Dunbabin, A. Grinham, and J. Udy, "An autonomous surface vehicle for water quality monitoring," in *Proc. Australasian Conf. Robotics and Automation*, Sydney, Australia, 2009, p. 13.

[21] M. Stealey, A. Singh, M. Batalin, B. Jordan, and W. Kaiser, "NIMSAQ: A novel system for autonomous sensing of aquatic environments," in *Proc. IEEE ICRA*, Pasadena, CA, 2008, pp. 621–628.

[22] D. F. Rogers and S. G. Satterfield (1980, July). B-spline surfaces for ship hull design *SIGGRAPH Comput. Graph.* [Online]. 14, pp. 211–217. Available: http://doi.acm.org/10.1145/965105.807494

[23] C. Samson and K. Ait-Abderrahim, "Feedback control of a nonholonomic wheeled cart in Cartesian space," in *Proc. IEEE ICRA*, Sacramento, CA, 1991, vol. 2, pp. 1136–1141.

[24] F. Pomerleau, S. Magnenat, F. Colas, M. Liu, and R. Siegwart, "Tracking a depth camera: Parameter exploration for fast ICP," in *Proc. IEEE/RSJ IROS*, San Francisco, CA, 2011, pp. 3824–3829.

***Gregory Hitz***, Autonomous Systems Laboratory, ETH Zurich, Switzerland. E-mail: gregory.hitz@mavt.ethz.ch.

***François Pomerleau***, Autonomous Systems Laboratory, ETH Zurich, Switzerland. E-mail: françois.pomerleau@mavt.ethz.ch.

***Marie-Ève Garneau***, Limnological Station Kilchberg, University of Zurich, Switzerland. E-mail: me.garneau@gmail.com.

***Cédric Pradalier***, Autonomous Systems Laboratory, ETH Zurich, Switzerland. E-mail: cédric.pradalier@mavt.ethz.ch.

***Thomas Posch***, Limnological Station Kilchberg, University of Zurich, Switzerland. E-mail: posch@limnol.uzh.ch.

***Jakob Pernthaler***, Limnological Station Kilchberg, University of Zurich, Switzerland. E-mail: pernthaler@limnol.uzh.ch.

***Roland Y. Siegwart***, Autonomous Systems Laboratory, ETH Zurich, Switzerland. E-mail: Roland.Siegwart@mavt.ethz.ch, rsiegwart@ethz.ch.